

Entropic force of a fluctuating semiflexible polymer exerted on a nanoparticle

Shi-Qiang Li(李世强), Yu-Shan Zheng(郑玉山), Xiao-Jing Wan(万晓静), and Kai Li(李凯)

Citation: Chin. Phys. B, 2026, 35 (**4**): 046101. DOI: 10.1088/1674-1056/ae2d31
http://cpb.iphy.ac.cn; http://iopscience.iop.org/cpb

What follows is a list of articles you may be interested in

Substrate tuned reconstructed polymerization of naphthalocyanine on Ag(110)

Qi Zheng(郑琦), Li Huang(黄立), Deliang Bao(包德亮), Rongting Wu(武荣庭), Yan Li(李彦), Xiao Lin(林晓), Shixuan Du(杜世萱), and Hong-Jun Gao(高鸿钧)

Chin. Phys. B, 2022, 31 (**1**): 018202. DOI: 10.1088/1674-1056/ac3500

Control on *β* conformation of poly(9,9-di-n-octylfluorene) via solvent annealing

Zhi Chao Zhang(张志超), Bing Yue Zhang(张丙悦), Yu Yan Weng(翁雨燕), Tian Hui Zhang(张天辉)

Chin. Phys. B, 2019, 28 (**7**): 076101. DOI: 10.1088/1674-1056/28/7/076101

Micro-track structure analysis for 100 MeV Si ions in CR-39 by using atomic force microscopy

Fang Mei-Hua (方美华), Wei Zhi-Yong (魏志勇), Zhang Zi-Xia (张紫霞), Zhu Li (朱立), Fu Yu (府宇), Shi Miao (石苗), Li Guang-Wu (黎光武), Guo Gang (郭刚)

Chin. Phys. B, 2013, 22 (**11**): 116105. DOI: 10.1088/1674-1056/22/11/116105

Entropic force of a fluctuating semiflexible polymer exerted on a nanoparticle

Shi-Qiang Li(李世强)[†], Yu-Shan Zheng(郑玉山)[†], Xiao-Jing Wan(万晓静), and Kai Li(李凯)[‡]

College of Mechanical Engineering, Xinjiang University, Urumqi 830002, *China*

(Received 17 September 2025; revised manuscript received 4 December 2025; accepted manuscript online 16 December 2025)

This study theoretically investigates the force exerted on a nanoparticle (NP) by a clamped semiflexible chain in solution. The force exerted by the semiflexible chain on the NP is related to the chain's conformational entropy, known as the entropic force. Under the weakly bending approximation, we derive an analytical formula for the entropic force using perturbation theory. This force can be divided into two components: parallel (f_ρ) and perpendicular (f_z, lifting the NP) to the initial vector at the clamped end. These two components are correlated with the local slope of the NP's cross-section, with the component f_z additionally linked to the local curvature. We compare the magnitude of force f_z with the Euler buckling threshold f_c. The study reveals that as the chain becomes more compressed, f_z initially peaks at a value exceeding the mechanical limit and subsequently decreases to a steady-state value lower than f_c. This behavior significantly differs from the entropic force derived under flat wall confinement. In three dimensions, f_z always stays below the Euler buckling threshold and in two dimensions it is larger than f_c for most of the parameter space.

Keywords: semiflexible chain, entropic force, perturbation theory, Euler buckling

PACS: 61.82.Pv, 82.35.Gh

DOI: 10.1088/1674-1056/ae2d31 **CSTR:** 32038.14.CPB.ae2d31

1. Introduction

The interaction between polymer chains and nanoparticles (NPs) is vital in multiple domains, including biological processes and material synthesis. For example, in biological processes[1–4] the interactions between receptors and ligands on the cell surface play a pivotal role in cellular signaling and recognition. Additionally, the interactions between proteins and NPs can alter the structure and functionality of proteins.[5–9] In material synthesis,[10–13] the interaction between polymer chains and NPs offers precise control over the assembly and arrangement of NPs, facilitating the design and synthesis of functionalized materials.

Typically, polymer chains form polymer brushes in the substrate to interact with NPs. Polymer brushes on substrates and their combination with NPs to create hybrid materials have extensive applications in various fields including life sciences and industrial production (e.g., catalysts, membranes and optoelectronic devices), due to their high thermodynamic stability.[14–18] The interaction between polymer brushes and NPs greatly influences the physical and mechanical properties of these materials. Theoretical studies, such as self-consistent field theory (SCFT)[19–24] and density functional theory (DFT),[25–29] have been widely used to investigate the forces exerted by polymer brushes on NPs and the phase diagrams of polymer brushes and NPs in hybrid materials.[30] Additionally, computer simulations and experimental investigations are conducted to validate these theoretical findings.[31–39]

The interaction between polymer chains and NPs remains a topic of ongoing research with some key challenges.[19,21,40–43] Most studies have primarily focused on the cluster effect of polymer chains on NPs, with limited quantification of the forces exerted by individual polymer chains on a single NP. Furthermore, existing theoretical models often employ ideal Gaussian chains for polymers, neglecting the inherent bending stiffness of the chains.[21,42,44,45] To understand the micromechanical properties of individual semiflexible polymer chains in relation to NPs, which are crucial for evaluating the macromechanical properties of hybrid materials, further investigations are necessary.

In solution, the configuration of polymer chains undergoes constant conformational changes in response to thermal perturbations, and the effect of conformational entropy needs to be taken into account in comparison with the mechanistic problem of buckling. The presence of NPs has a significant impact on the conformational entropy of polymer chains, leading to a confinement-induced reduction of entropy and the emergence of an entropic force.[15,46,47] Understanding the entropic force exerted by a single polymer chain on the surface of an NP is the main objective of this study. The entropic force is directly linked to the probability distribution of the chain in space. For a flexible chain, solving for the entropic force is relatively straightforward. Flexible chains are usually modelled as Gaussian chains, which display diffusion-like behavior in terms of probability distributions, and allow for analytical so-

[†]These authors contributed equally to this work.

[‡]Corresponding author. E-mail: likai@xju.edu.cn

© 2026 Chinese Physical Society and IOP Publishing Ltd. All rights, including for text and data mining, AI training, and similar technologies, are reserved.

lutions of the entropic force under specific constraints (e.g., planar, spherical, cylindrical) by solving the diffusion equation with appropriate boundary conditions.[44,48,49] In the case of flexible chains, the entropic force is only related to the position vector. For semiflexible chains, the distribution of chain segments is influenced by their positions and tangential vectors, posing significant theoretical challenges in finding analytical solutions. As a result, most existing theoretical studies have focused on flat wall confinement.[50–52] For stiff chains, the entropic force exerted on a plane exceeds the Euler buckling threshold in two-dimensional systems, while consistently remaining lower in three-dimensional systems.[51] The initial angle of the clamped end also affects the entropic force. Bayati *et al.*[53] calculated the entropic force of a clamped semiflexible chain exerted on a rough plane by using perturbation theory. However, this derivation did not consider the impact of the local slope of the surface on the entropic force in the direction perpendicular to the plane.

Thus, there has been limited theoretical exploration of the entropic force exerted by a single clamped semiflexible chain on an NP. Using perturbation theory, this paper aims to theoretically investigate the force exerted on a NP by a clamped semiflexible chain in solution. It is important to note that the entropic force is influenced by the local slope and curvature of the NP's cross-section. In our calculations, the wormlike chain (WLC) model is taken as the theoretical model of a semiflexible chain. This widely used theoretical model for semiflexible polymers was proposed by Kratky and Porod.[54] The WLC model has two length scales: contour length L and persistence length p. The persistence length p is a length scale beyond which thermal fluctuations erase any memories about the initial direction of the polymer. The ratio L/p can be used to classify polymers into flexible ($L/p \gg 1$), semiflexible ($L/p \sim 1$) and stiff ($L/p \ll 1$) polymers. Our model is based on a semiflexible chain. When $L/p \ll 1$ the chain exhibits stiffness and can be compared with the Euler buckling threshold for plane constraints.

The paper is organized as follows. In Section 2, we introduce a toy model concerning a fluctuating semiflexible polymer with one end clamped on the plane and the other end confined by the surface of a stiff NP. We give an analytical expression for the entropic forces exerted on the NP by a single polymer chain through perturbation theory. In Section 3, we give quantitative results and discuss the entropic forces exerted by a stiff polymer chain on the NP. In Section 4, a summary and outlook are briefly given.

2. Model and theory

2.1. Slope and curvature affect entropic forces

The WLC model, as one of the theoretical models for polymer chains, is commonly used in the study of semiflexible chains. This model provides an excellent fit to experimental data when characterizing the statistical mechanical behavior of semiflexible chains under stretching, compression or geometric constraint. The configuration of a semiflexible polymer is described by a position vector $\boldsymbol{r}(s)$ and a tangent vector $\boldsymbol{u}(s)$. According to the WLC model, each differential segment is constrained to be inextensible, which means $|\boldsymbol{u}(s)| = 1$. s is the arc length along the backbone and $s \in [0, L]$. The bending energy is given by

$$\beta H_0 = \frac{p}{2}\int_0^L \left(\frac{\partial \boldsymbol{u}}{\partial s}\right)^2 \mathrm{d}s, \tag{1}$$

where $\beta = 1/k_{\mathrm{B}}T$.

Figure 1(a) shows a schematic diagram of the entropic force exerted by a stiff polymer chain on an NP of radius R. The height of the bottom of the NP from the plane is h, and the initial direction of the clamped end ($s = 0$) of the chain is perpendicular to the plane. The other end ($s = L$) is thermally disturbed near the NP. We establish a cylindrical coordinate system (ρ, z, φ) at the initial end of the polymer chain. The entropic force exerted by the chain on the NP can be decomposed into three components: perpendicular to the plane f_z, tangential to NP surface f_φ and translating the NP f_ρ.

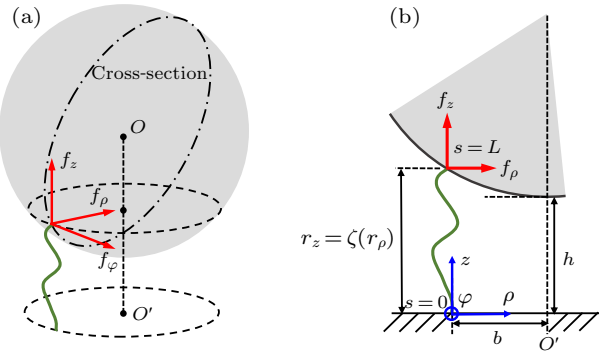


Fig. 1. The force exerted on NP by a stiff polymer chain (a). We choose the $O\rho Z$ plane as the coordinate system to be established for the theoretical study (b) and the φ-direction is chosen to be tangential to the surface of the sphere.

In order to mathematically calculate the entropic forces exerted on the NP by a stiff polymer chain, we start with the effective Hamiltonian

$$\beta H_1 = \frac{p}{2}\int_0^L \left(\frac{\partial \boldsymbol{u}}{\partial s}\right)^2 \mathrm{d}s + \frac{V[\boldsymbol{r}(s)]}{k_{\mathrm{B}}T}, \tag{2}$$

where $V[\boldsymbol{r}(s)]$ represents the hard-wall-confining potential due to the NP surface. It can be written as

$$V[\boldsymbol{r}(s)] = \begin{cases} 0, & r_z(L) < \zeta\left[r_\rho(L)\right], \\ \infty, & r_z(L) \geq \zeta\left[r_\rho(L)\right], \end{cases} \tag{3}$$

where $\zeta(r_\rho)$ is the distance from the sphere along the z-axis direction (Fig. 1(b)). For ease of presentation, we omit L and write $r_z(L)$ and $r_\rho(L)$ as r_z and r_ρ.

The function $\zeta(r_\rho)$ is related only to the distance from the fixed end of the chain to O' (the projection of the center of

the sphere on the plane). Due to the symmetry of the physical problem, $\zeta(r_\rho)$ is independent of the angle φ, therefore we only consider entropic forces in the z and ρ directions. For the convenience of subsequent mathematical calculations, we have chosen the fixed end of the chain as the coordinate origin of the coordinate system (see Fig. 1(b)). $\zeta(r_\rho)$ can be written as

$$\zeta(r_\rho) = -\sqrt{R^2 - (r_\rho - b)^2} + R + h \tag{4}$$

by the equation of a circle. b is the distance from O' to the clamped end of the polymer.

The ensemble average for the force exerted by the polymer tip on the NP reads[55]

$$\langle f_{\rho,z}(\zeta)\rangle = \frac{1}{\beta}\frac{\partial}{\partial r_{\rho,z}}\ln Z. \tag{5}$$

Here Z is the partition function related to the statistical properties of the system and can be written in the form of path integral

$$Z = \int \mathcal{D}[\boldsymbol{r}(s)]\exp[-\beta H_1]. \tag{6}$$

We choose the measure of the functional integral in such a way that the partition function for a free polymer ($V[\boldsymbol{r}(s)] = 0$) is normalized to 1.

The solution of the entropic force requires us to evaluate the functional integrals in Eq. (6). Here we are interested in studying the confinement effects due to a wall that is slightly deformed from a flat wall, which means the radius of the NP is sufficiently large. Therefore, the partition function in Eq. (6) can be decomposed into two parts. One is the partition function Z_0 corresponding to a fluctuating WLC confined by a flat wall. The other is the small quantity ΔZ caused by the degree of curvature of the NP surface. We expand the logarithm of the partition function in Eq. (6) at $Z = Z_0$. The leading order of the expansion can be written as

$$\begin{aligned}\ln Z &= \ln(Z_0 - \Delta Z) = \ln Z_0 - \Delta Z\frac{\partial \ln Z}{\partial Z}\bigg|_{Z=Z_0} \\ &= \ln Z_0 - \frac{\Delta Z}{Z_0}.\end{aligned} \tag{7}$$

In the stiff limit, the persistence length p is sufficiently large compared with the contour length L, which implies that back-turns of the polymer chain are almost impossible. This allows us to express the hard wall potential energy $V[\boldsymbol{r}(s)]$ in terms of a step function for further mathematical treatment in Eq. (3)

$$\exp(-\beta V[\boldsymbol{r}(s)]) = \Theta[\zeta(r_\rho) - r_z]. \tag{8}$$

The Heaviside step function $\Theta[\zeta(r_\rho) - r_z]$ indicates that only those configurations are counted when the position of the polymer tip is under the NP surface. Now for a wall that is slightly deformed from a reference flat configuration, the step function can be expanded around $r_\rho = 0$ as

$$\begin{aligned}\Theta[\zeta(r_\rho) - r_z] \approx\ & \Theta(\zeta_0 - r_z) - Q\delta(\zeta_0 - r_z) \\ & + \frac{1}{2}S^2\delta'(\zeta_0 - r_z)r_\rho^2,\end{aligned} \tag{9}$$

$$Q = Sr_\rho + \frac{1}{2}Cr_\rho^2, \tag{10}$$

where $\zeta_0 = \zeta(0)$ is the projected distance of the entire chain in the z-direction. S and C are the slope and curvature of the surface

$$S = -\frac{\partial\zeta}{\partial r_\rho}\bigg|_{r_\rho=0}, \quad C = -\frac{\partial^2\zeta}{\partial r_\rho^2}\bigg|_{r_\rho=0}. \tag{11}$$

The expressions for ζ_0, S and C can be obtained from Eq. (4). The Taylor expansion of Eq. (4) at point $r_\rho = 0$ can be expressed as

$$\begin{aligned}\zeta(r_\rho) \approx\ & -\sqrt{R^2 - b^2} + h + R - \frac{b\sqrt{R^2 - b^2}}{R^2 - b^2}r_\rho \\ & + \frac{R^2\sqrt{R^2 - b^2}}{2(R^2 - b^2)^2}r_\rho^2,\end{aligned} \tag{12}$$

which implies $\zeta_0 = -\sqrt{R^2 - b^2} + h + R$. The slope S and curvature C of the cross section are

$$S = \frac{b\sqrt{R^2 - b^2}}{R^2 - b^2}, \quad C = -\frac{R^2\sqrt{R^2 - b^2}}{(R^2 - b^2)^2}. \tag{13}$$

Combining Eqs. (6), (8), and (9), we find that Z_0 is the partition function for a polymer confined by a flat wall at a distance ζ_0 from the origin in the z-direction, and can be written as

$$Z_0 = \int \mathcal{D}[\boldsymbol{r}(s)]\exp[-\beta H_0]\Theta(\zeta_0 - r_z). \tag{14}$$

The function ΔZ that determines the curvature and slope of the surface contribution is given by

$$\Delta Z = \Delta Z_1 + \Delta Z_2, \tag{15}$$

$$\Delta Z_1 = \int \mathcal{D}[\boldsymbol{r}(s)]\exp[-\beta H_0]\left(Sr_\rho + \frac{1}{2}Cr_\rho^2\right)\delta(\zeta_0 - r_z), \tag{16}$$

$$\Delta Z_2 = \int \mathcal{D}[\boldsymbol{r}(s)]\exp[-\beta H_0]\left(-\frac{1}{2}S^2\delta'(\zeta_0 - r_z)r_\rho^2\right). \tag{17}$$

The expression for ΔZ implies that the entropic force exerted by the polymer chain on the NP is related to S and C. Combining Eqs. (5), (7), (14) and (15), the force exerted by a semiflexible polymer chain on the NP in the z-direction can be written as

$$\langle f_z\rangle = k_\mathrm{B}T\frac{1}{Z_0}\left(\frac{\partial Z_0}{\partial r_z} - \frac{\partial\Delta Z}{\partial r_z} + \Delta Z\frac{\partial \ln Z_0}{\partial r_z}\right). \tag{18}$$

We note that Z_0 is independent of r_ρ, and that for an entropic force in the ρ-direction, there is only one term

$$\langle f_\rho\rangle = -k_\mathrm{B}T\frac{1}{Z_0}\frac{\partial\Delta Z}{\partial r_\rho}. \tag{19}$$

Now we are in a position to calculate the partition function Z_0 and ΔZ. In the next section, we will give the analytical expression for the partition function by using modal analysis in the stiff chain limit.

2.2. The stiff chain limit: modal analysis

In order to calculate the partition function in path integral form, we will use Fourier mode analysis and the weakly bending approximation. When the persistence length p is large enough compared with the total contour length L, the undulation of the chain due to thermal fluctuation will be small. Combining the inextensible condition $|\boldsymbol{u}(s)|=1$ of the WLC model, the variation of the tangential vector along the chain length can be written as[53]

$$\frac{\partial \boldsymbol{u}}{\partial s} \approx \frac{\partial \boldsymbol{u}_{\perp}}{\partial s} = \frac{\partial u_{\rho}}{\partial s}\boldsymbol{\rho} + \frac{\partial u_{\varphi}}{\partial s}\boldsymbol{\varphi}. \tag{20}$$

The clamped end of the polymer in our system is parallel to the z-axis and the other end is free. The boundary conditions at the ends of the polymer are

$$u_{\rho}(0) = u_{\varphi}(0) = 0, \quad \dot{u}_{\rho}(L) = \dot{u}_{\varphi}(L) = 0. \tag{21}$$

The forces on this polymer chain are similar to a cantilever beam model in mechanics, with one end constrained and the other free. Therefore, the boundary conditions are also consistent. The boundary conditions at the ends of the polymer allow us to perform a Fourier series expansion

$$\begin{aligned} u_{\rho}(s) &= \sum_{k=1}^{\infty} a_{\rho,k} \sin\left(\lambda_k \frac{s}{L}\right), \\ u_{\varphi}(s) &= \sum_{k=1}^{\infty} a_{\varphi,k} \sin\left(\lambda_k \frac{s}{L}\right), \end{aligned} \tag{22}$$

with eigenvalues $\lambda_k = \frac{\pi}{2}(2k-1)$.

The Hamiltonian of the free WLC model can be expressed as

$$\beta H_0 = \frac{p}{4L}\sum_{k=1}^{\infty} \lambda_k^2 \left(a_{\rho,k}^2 + a_{\varphi,k}^2\right). \tag{23}$$

The fluctuation end vector of the polymer chain reads

$$r_{\rho} \approx \sum_{k=1}^{\infty} a_{\rho,k} \int_0^L \mathrm{d}s \sin(\lambda_k s/L) = L\sum_{k=1}^{\infty} \lambda_k^{-1} a_{\rho,k}, \tag{24}$$

$$\begin{aligned} r_z &= \int_0^L u_z(s)\,\mathrm{d}s \approx L - \frac{1}{2}\int_0^L \boldsymbol{u}_{\perp}^2\,\mathrm{d}s \\ &= L - \frac{L}{4}\sum_{k=1}^{\infty}\left(a_{\rho,k}^2 + a_{\varphi,k}^2\right). \end{aligned} \tag{25}$$

The partition function Z_0 under flat wall confinement can be obtained from the moment-generating function and the Fourier series, which can be expressed as[51]

$$Z_0(\zeta_0) = 2\sum_{k=1}^{\infty} (-1)^{k+1} \lambda_k^{-1} \exp\left(-\eta\lambda_k^2 p/L^2\right), \tag{26}$$

Z_0 is a function of ζ_0 and $\eta = L - \zeta_0$ is the stored length. This is because for a fixed distance ensemble, the quantity Z_0 measures the number of configurations obeying hard-wall confinement. Upon using Eq. (26) one may write the entropic force exerted by a clamped chain on the flat wall as

$$\langle f_0 \rangle = k_{\mathrm{B}} T \frac{\partial}{\partial \zeta_0} \ln Z_0. \tag{27}$$

The partition function ΔZ means that the curvature and slope contribution contain the Dirac function $\delta(\zeta_0 - r_z)$ and its derivatives $\delta'(\zeta_0 - r_z)$. Analytical calculation of the function ΔZ starts from the Laplace transform to eliminate these functions. Up to the leading order of deformation, all integrals are Gaussian and can be analytically performed. The theoretical formula for the final result for ΔZ is

$$\begin{aligned} \Delta Z(\zeta_0) =\ & CL\sum_{k=1}^{\infty} \lambda_k^{-4} \sum_{l\neq k} \lambda_l^2 \exp\left(-\eta\lambda_l^2 p/L^2\right) \left(1-\frac{\lambda_l^2}{\lambda_k^2}\right)^{-2} \prod_{m\neq k,l}\left(1-\frac{\lambda_l^2}{\lambda_m^2}\right)^{-1} \\ & - CL\sum_{k=1}^{\infty} \exp\left(-\eta\lambda_k^2 p/L^2\right) \prod_{m\neq k}\left(1-\frac{\lambda_k^2}{\lambda_m^2}\right)^{-1} \left[-\frac{p}{L^2}\eta + \sum_{l\neq k}\lambda_l^{-2}\left(1-\frac{\lambda_k^2}{\lambda_l^2}\right)^{-1}\right] \\ & - \frac{S^2 p}{L}\sum_{k=1}^{\infty} \lambda_k^{-4} \sum_{l\neq k} \lambda_l^4 \exp\left(-\eta\lambda_l^2 p/L^2\right) \left(1-\frac{\lambda_l^2}{\lambda_k^2}\right)^{-2} \prod_{m\neq k,l}\left(1-\frac{\lambda_l^2}{\lambda_m^2}\right)^{-1} \\ & + \frac{S^2 p}{L}\sum_{k=1}^{\infty} \exp\left(-\eta\lambda_k^2 p/L^2\right) \prod_{m\neq k}\left(1-\frac{\lambda_k^2}{\lambda_m^2}\right)^{-1} \left(\frac{L^2 - \eta\lambda_k^2 p}{L^2}\right) \\ & + \frac{S^2 p}{L}\sum_{k=1}^{\infty} \exp\left(-\eta\lambda_k^2 p/L^2\right) \prod_{m\neq k}\left(1-\frac{\lambda_k^2}{\lambda_m^2}\right)^{-1} \left[\lambda_k^2 \sum_{l\neq k}\lambda_l^{-2}\left(1-\frac{\lambda_k^2}{\lambda_l^2}\right)^{-1}\right]. \end{aligned} \tag{28}$$

Details of the calculations are given in Appendix A.

We have now derived the partition function $Z = Z_0 - \Delta Z$. According to the properties of the Dirac function and Eq. (18), the force in the z-direction can be written as

$$\langle f_z(\zeta_0)\rangle = k_B T \frac{1}{Z_0}\left(\frac{\partial Z_0}{\partial \zeta_0} - \frac{\partial \Delta Z}{\partial \zeta_0} + \Delta Z \frac{\partial \ln Z_0}{\partial \zeta_0}\right). \quad (29)$$

Combining Eqs. (16), (17) and (19), note that ΔZ appears as the primary term of r_ρ in the path integral after the derivation of r_ρ and does not contribute to the integral in the following modal analysis. Thus, the entropic force in the ρ-direction can be simplified as (for details of the calculations see Appendix B)

$$\langle f_\rho(\zeta_0)\rangle = -k_B T \frac{S}{Z_0}\frac{\partial Z_0}{\partial \zeta_0}. \quad (30)$$

Finally, we have given the perturbation results for the entropic force exerted by a WLC on the NP. This allows us to explicitly study the entropic forces and their dependence on the parameters of our system. In the next subsection, we normalize f_z and f_ρ using the classical Euler buckling threshold and give a discussion of our main results.

3. Discussion

In the previous section, we presented theoretical results for the entropic force exerted on an NP by a semiflexible polymer chain clamped at one end. Unlike flat wall confinement, the entropic force of spherical confinement corresponds to an NP having not only a component f_z in the vertical direction but also a horizontal component f_ρ in the horizontal direction due to the asymmetry of the probability distribution caused by the influence of the curved surface. A prefactor identical to the classical Euler buckling threshold[56]

$$f_c = \frac{\pi^2 p}{4L^2} k_B T, \quad (31)$$

is required to make the components of force non-dimensional.

Figure 2(a) shows the normalized entropic force exerted by a semiflexible chain in the direction z on the NP for the parameters that we have chosen ($p/L = 10$). As the radius of the NP increases or the location b decreases, the geometrically constrained surface becomes flat and f_z gradually approaches the entropic force of a flat wall f_0 (dashed line) in Eq. (18). It is surprising that f_z has a peak value greater than the classical Euler buckling threshold for smaller compression ratios. For a larger compression ratio ($\eta/L \geq 0.05$), f_z converges to a stable value but is smaller than f_c. This is because the z-direction entropic force is related to the slope S of the NP section. The sloping planes allow more configurations to appear for individual polymer chains compared with flat wall confinement.

To show how the curved wall enhances f_z, we have used the corresponding force for a flat wall to make a nondimensional force f_z/f_0 with a change in the compression ratio η/L (Fig. 3). When the polymer chain is fully extended ($\eta = 0$), at this point no force is applied to the NP ($f_0 = 0$), which leads to divergence at $\eta = 0$. However, as η/L gradually increases, the vertical component f_z of the entropic force gradually approaches f_0. We notice that the effect caused by the curved surface focuses on the small compression case η/L $\left(\eta/L \leq 1.5\times10^{-3}\right)$. f_z converges to a stable value less than f_0 when η/L becomes progressively larger. The horizontal coordinates η/L in Figs. 2 and 3 are normalized for η.

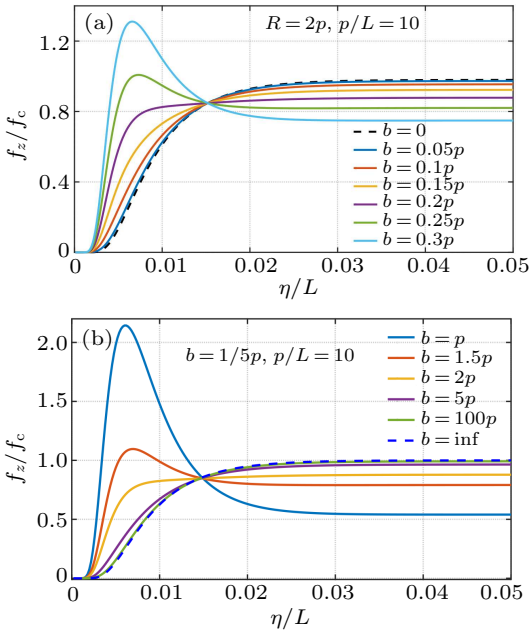


Fig. 2. Normalized force f_z varies with the compression ratio η/L with different locations b (a) or NP radii R (b). In the figure, we set the parameters $p/L = 10$ and normalize force f_z with the classical Euler buckling threshold.

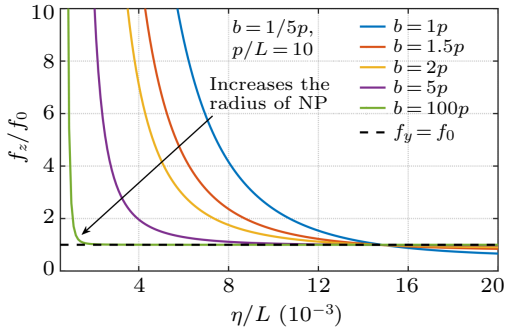


Fig. 3. Variation of the ratio of f_z and f_0 with compression ratio η/L.

The force f_ρ exerted on the NP by the polymer chain in the ρ direction is only related to the slope S of cross-section. In Fig. 4 we plot the normalized force exerted on the wall along the ρ-direction with the variation of polymer chain location b (Fig. 4(a)) and NP radius R (Fig. 4(b)). For a constant parameter $p/L = 50$, increasing the location b of the polymer's clamped end or decreasing the persistence length leads to f_ρ increasing. This is mainly due to the linear relationship between f_ρ and S in Eq. (30). At the same time, the force f_ρ in the ρ-direction will increase with increase in the compression parameter η.

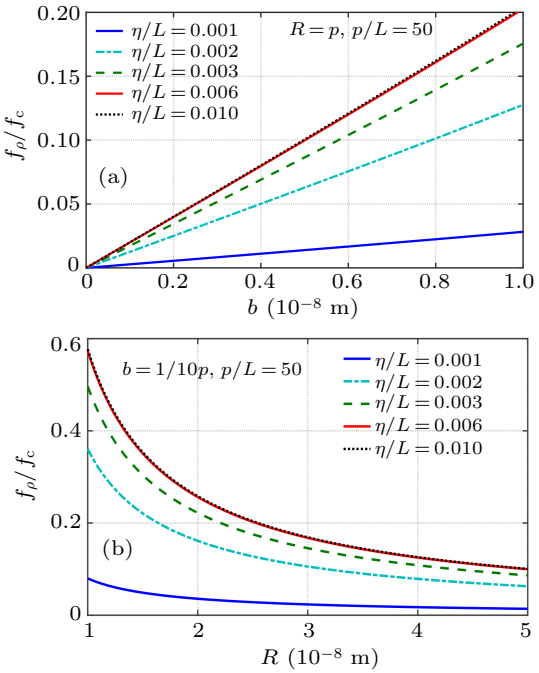


Fig. 4. Normalized force f_ρ varies with polymer chain location b (a) and NP radius R (b). The parameter used is $p/L=50$. Different color curves correspond to different compression ratios η/L.

4. Summary and outlook

In summary, we have theoretically analyzed the entropic forces exerted by a semiflexible polymer on an NP surface. We divide the partition function Z of our system by perturbation theory into a first term Z_0 and a small amount ΔZ. Z_0 represents the partition function of the system under flat wall confinement, while ΔZ is the contribution of the spherical slope and curvature. In the limit of the weakly bending approximation, we have derived the first-order nontrivial corrections of the partition function and found that ΔZ is related to slope S and local curvature C of the NP cross section. The entropic force can be divided into a parallel component (f_ρ) and a perpendicular component (f_z, lifting NP) to the initial vector at the graft end. The entropic force f_z of the polymer chain on the flat wall in the three-dimensional case is always smaller than the Euler buckling threshold f_c. However, when the flat wall becomes a curved surface, the addition of a slope and the curvature of the curve causes a peak in the entropic force greater than f_c. The difference between the forces f_z and f_c is due to the decrease in conformational entropy of the polymer chain caused by the presence of an NP.

Two important complexities that we have not addressed here are related to electrostatic effects and the effects of polymer chain excluded volume. This is because polymer brushes usually have a net charge[57,58] and the polymer chains that make up the bristles are distributed at a large density, requiring consideration of the effect of exclusion of volume effects on entropic forces.[59,60] A complete theory for entropic forces should also incorporate these effects. In this study, we only considered the interaction of a single polymer chain with an NP, and in practice the effects of other chains need to be taken into account, including chain-to-chain interactions and multi-chain interactions with the NP, which must be considered in subsequent studies.

Appendix A: Derivation of ΔZ

A1. Derivation of ΔZ_1

In this appendix, we solve the partition function ΔZ by modal analysis and Laplace transform. Here we decompose ΔZ into two parts ΔZ_1 and ΔZ_2. ΔZ_1 contains the Dirac function and can be written as

$$\Delta Z_1=\int \mathcal{D}[\boldsymbol{r}(s)]\exp(-\beta H_0)\left(Sr_\rho+\frac{1}{2}Cr_\rho^2\right)\delta(\zeta_0-r_z). \quad \text{(A1)}$$

To eliminate the Dirac function $\delta(\zeta_0-r_z)$, we first define the Laplace transform as

$$P_1(f)=\int_0^{2L}\exp(-\beta f\eta)\Delta Z_1\,\mathrm{d}\eta\approx\int_0^{\infty}\exp(-\beta f\eta)\Delta Z_1\,\mathrm{d}\eta, \quad \text{(A2)}$$

and $\eta=L-\zeta_0$ is the stored length. Since stiff chain configurations with large compression are rather unlikely, the upper limit of integration can be approximated to infinity by $2L$. Substituting Eq. (A1) into Eq. (A2) we obtain

$$P_1(f)=\int\mathcal{D}[\boldsymbol{r}(s)]\exp[-\beta H_0-\beta f(L-r_z)]\times\left(Sr_\rho+\frac{1}{2}Cr_\rho^2\right), \quad \text{(A3)}$$

βH_0, r_ρ and r_z are expressed as Fourier series in the main text. The following path integral form is related to the Fourier coefficient and all integrals are Gaussian and can be analytically done. According to the Gaussian integral $\int_{-\infty}^{+\infty}\exp\left(-1/2ax^2\right)x\mathrm{d}x=0$, we find that the integral in Eq. (A3) associated with S does not contribute to the integral. Then $P_1(f)$ can be written as

$$P_1(f)=\frac{C}{2}\int\mathcal{D}[\boldsymbol{r}(s)]\exp[-\beta H_0-\beta f(L-r_z)]r_\rho^2. \quad \text{(A4)}$$

The path integral can be written as

$$\begin{aligned}P_1(f)&=\frac{C}{2}\int\prod_{i=1}^{\infty}\frac{\mathrm{d}a_{\rho,i}\mathrm{d}a_{\varphi,i}}{\mathcal{N}_i}\exp\left[-\frac{a_{\rho,i}^2+a_{\varphi,i}^2}{4}\left(\frac{p}{L}\lambda_i^2+\beta fL\right)\right]\sum_{k=1}^{\infty}L^2\lambda_k^{-2}a_{\rho,k}^2\\&=\frac{C}{2}\sum_{k=1}^{\infty}\left\{\int\prod_{i=1}^{\infty}\frac{\mathrm{d}a_{\varphi,i}}{\sqrt{\mathcal{N}_i}}\exp\left[-\frac{1}{2}\left(\frac{1}{2}\frac{p}{L}\lambda_i^2+\frac{1}{2}\beta fL\right)a_{\varphi,i}^2\right]\right\}\left\{\int\prod_{i=1}^{\infty}\frac{\mathrm{d}a_{\rho,i}}{\sqrt{\mathcal{N}_i}}\exp\left[-\frac{1}{2}\left(\frac{1}{2}\frac{p}{L}\lambda_i^2+\frac{1}{2}\beta fL\right)a_{\rho,i}^2\right]L^2\lambda_k^{-2}a_{\rho,k}^2\right\}.\end{aligned} \quad \text{(A5)}$$

$\mathcal{N}_i = 4\pi L/\lambda_i^2 p$ is the normalization factor of the path integral. The final result of the integral is in the form of a series

$$P_1(f) = \frac{C}{2}\sum_{k=1}^{\infty}\frac{2L^3}{p\lambda_k^4}\left(1+\frac{\beta f L^2}{p\lambda_k^2}\right)^{-1}\prod_{i=1}^{\infty}\left(1+\frac{\beta f L^2}{\lambda_i^2 p}\right)^{-1}. \tag{A6}$$

Now we can obtain ΔZ_1 by performing the inverse Laplace transform on $P_1(f)$

$$\begin{aligned}\Delta Z_1(\zeta_0) &= \int_{-\mathrm{i}\infty}^{\mathrm{i}\infty}\frac{\beta}{2\pi\mathrm{i}}\exp(\beta f\eta)P_1(f)\,\mathrm{d}f\\ &= C\beta\sum_{k=1}^{\infty}\frac{1}{2\pi\mathrm{i}}\int_{-\mathrm{i}\infty}^{\mathrm{i}\infty}\exp(\beta f\eta)\frac{L^3}{p\lambda_k^4}\left(1+\frac{\beta f L^2}{p\lambda_k^2}\right)^{-2}\\ &\quad\times\prod_{i\neq k}^{\infty}\left(1+\frac{\beta f L^2}{\lambda_i^2 p}\right)^{-1}\mathrm{d}f.\end{aligned} \tag{A7}$$

We can compute Eq. (A7) by means of the residue theorem

$$\frac{1}{2\pi\mathrm{i}}\int_{-\mathrm{i}\infty}^{\mathrm{i}\infty}F(f)\,\mathrm{d}f = \sum\mathrm{Res}\left[F(f), f_p\right], \tag{A8}$$

where f_p is a singularity. The final results can be written as

$$\begin{aligned}\Delta Z_1(\zeta_0) &= -CL\sum_{k=1}^{\infty}\exp\left(-\eta\lambda_k^2 p/L^2\right)\\ &\quad\times\prod_{m\neq k}\left(1-\frac{\lambda_k^2}{\lambda_m^2}\right)^{-1}\left[-\frac{p}{L^2}\eta+\sum_{l\neq k}\lambda_l^{-2}\left(1-\frac{\lambda_k^2}{\lambda_l^2}\right)^{-1}\right]\\ &\quad+CL\sum_{k=1}^{\infty}\lambda_k^{-4}\sum_{l\neq k}\lambda_l^2\exp\left(-\eta\lambda_l^2 p/L^2\right)\\ &\quad\times\left(1-\frac{\lambda_l^2}{\lambda_k^2}\right)^{-2}\prod_{m\neq k,l}\left(1-\frac{\lambda_l^2}{\lambda_m^2}\right)^{-1}.\end{aligned} \tag{A9}$$

A2. Derivation of ΔZ_2

The derivation of ΔZ_2 is similar to that of ΔZ_1. We consider the transformation of ΔZ_2 as

$$P_2(f) = \int_{-L}^{L}\mathrm{d}\zeta_0\exp\left[-\beta f(L-\zeta_0)\right]\Delta Z_2. \tag{A10}$$

For the derivative of the Dirac function $\delta'(x)$, we have

$$\int_{-\infty}^{\infty}f(x)\cdot\delta'(x-a)\,\mathrm{d}x = -f'(a). \tag{A11}$$

Then Eq. (A10) can be written as

$$P_2(f) = \frac{S^2}{2}\beta f\int\mathcal{D}[\boldsymbol{r}(s)]\exp\left[-\beta H_0-\beta f(L-r_z)\right]r_\rho^2. \tag{A12}$$

The result of the integration has been given in Eq. (A6), and we can obtain

$$P_2(f) = S^2\beta f\sum_{k=1}^{\infty}\frac{L^3}{p\lambda_k^4}\left(1+\frac{\beta f L^2}{p\lambda_k^2}\right)^{-1}\prod_{i=1}^{\infty}\left(1+\frac{\beta f L^2}{\lambda_i^2 p}\right)^{-1}. \tag{A13}$$

Upon performing the inverse Laplace transform, one obtains

$$\begin{aligned}\Delta Z_2(\zeta_0) &= -\frac{S^2 p}{L}\sum_{k=1}^{\infty}\lambda_k^{-4}\sum_{l\neq k}\lambda_l^4\exp\left(-\eta\lambda_l^2 p/L^2\right)\\ &\quad\times\left(1-\frac{\lambda_l^2}{\lambda_k^2}\right)^{-2}\prod_{m\neq k,l}\left(1-\frac{\lambda_l^2}{\lambda_m^2}\right)^{-1}\\ &\quad+\frac{S^2 p}{L}\sum_{k=1}^{\infty}\exp\left(-\eta\lambda_k^2 p/L^2\right)\prod_{m\neq k}\left(1-\frac{\lambda_k^2}{\lambda_m^2}\right)^{-1}\\ &\quad\times\left[\frac{L^2-\eta\lambda_k^2 p}{L^2}+\lambda_k^2\sum_{l\neq k}\lambda_l^{-2}\left(1-\frac{\lambda_k^2}{\lambda_l^2}\right)^{-1}\right].\end{aligned} \tag{A14}$$

Finally, the partition function ΔZ can be obtained from the sum of ΔZ_1 and ΔZ_2 as in the main text.

Appendix B: Derivation of f_ρ

In this section, we give the exact derivation of Eqs. (19)–(30). We first define $G = \partial\Delta Z/\partial r_\rho$. G can be divided into two parts defined as

$$\begin{aligned}G_1 &= \frac{\partial\Delta Z_1}{\partial r_\rho}\\ &= \int\mathcal{D}[\boldsymbol{r}(s)]\exp\left[-\beta H_0\right]\left(S+Cr_\rho\right)\delta(\zeta_0-r_z),\end{aligned} \tag{B1}$$

$$\begin{aligned}G_2 &= \frac{\partial\Delta Z_2}{\partial r_\rho}\\ &= \int\mathcal{D}[\boldsymbol{r}(s)]\exp\left[-\beta H_0\right]\left(-S^2\delta'(\zeta_0-r_z)r_\rho\right),\end{aligned} \tag{B2}$$

corresponding to ΔZ_1 and ΔZ_2, respectively.

We can use the Laplace transform to eliminate the Dirac function as

$$P_3(f) = \int\mathcal{D}[\boldsymbol{r}(s)]\exp\left[-\beta H_0-\beta f(L-r_z)\right]\left(S+Cr_\rho\right), \tag{B3}$$

$$P_4(f) = S^2\beta f\int\mathcal{D}[\boldsymbol{r}(s)]\exp\left[-\beta H_0-\beta f(L-r_z)\right]r_\rho. \tag{B4}$$

The path integrals in the above equations can be obtained by Fourier series and Gaussian integrals. Combining the Gaussian integral $\int_{-\infty}^{+\infty}x\exp\left(-1/2ax^2\right)\mathrm{d}x = 0$ and the expression for $r_\rho = L\sum_{k=1}^{\infty}\lambda_k^{-1}a_{\rho,k}$, we note that the linear term with respect to r_ρ does not contribute to the path integral. G can be expressed in a simplified form as

$$G = G_1+G_2 = S\int\mathcal{D}[\boldsymbol{r}(s)]\exp\left[-\beta H_0\right]\delta(\zeta_0-r_z). \tag{B5}$$

According to the expression of the Heaviside step function and Dirac function,

$$\frac{\partial}{\partial\zeta_0}\Theta(\zeta_0-r_z) = \delta(\zeta_0-r_z). \tag{B6}$$

Equation (B5) can be written as

$$G = S\frac{\partial\int\mathcal{D}[\boldsymbol{r}(s)]\exp\left[-\beta H_0\right]\Theta(\zeta_0-r_z)}{\partial\zeta_0} = S\frac{\partial Z_0}{\partial\zeta_0}. \tag{B7}$$

Thus f_ρ in Eq. (19) can be rewritten as

$$\langle f_\rho(\zeta_0)\rangle = -k_{\mathrm{B}}T\frac{S}{Z_0}\frac{\partial Z_0}{\partial \zeta_0} \tag{B8}$$

in the main text.

Acknowledgements

This work was financially supported by Xinjiang Autonomous Region Science and Technology Programme of China (Grant No. 2024B04007-2), Xinjiang Tianchi PhD Project (Grant No. TCBS202113), the Natural Science Foundation of Xinjiang Autonomous Region of China (Grant No. 2022D01C34), and Xinjiang Basic Research Funds for Universities (Grant No. XJEDU2022P017). The authors thank Professor Ji-Zeng Wang for his revision and suggestions.

References

[1] Moore N W and Kuhl T L 2006 *Biophys. J.* **91** 1675
[2] Moore N W, Mulder D J and Kuhl T L 2008 *Langmuir* **24** 1212
[3] Bauer M, Kékicheff P, Iss J, Fajolles C, Charitat T, Daillant J and Marques C M 2015 *Nat. Commun.* **6** 8117
[4] Bell S and Terentjev E M 2017 *Macromolecules* **50** 8810
[5] De Kruif C G and Tuinier R 2001 *Food Hydrocoll.* **15** 555
[6] Lynch I and Dawson K A 2008 *Nano Today* **3** 40
[7] Mahmoudi M, Lynch I, Ejtehadi M R, Monopoli M P, Bombelli F B and Laurent S 2011 *Chem. Rev.* **111** 5610
[8] Chakraborty S, Joshi P, Shanker V, Ansari Z A, Singh S P and Chakrabarti P 2011 *Langmuir* **27** 7722
[9] Huang R, Carney R P, Stellacci F and Lau B L 2013 *Nanoscale* **5** 6928
[10] Perumal S 2022 *Polymers* **14** 5449
[11] Grubbs R B 2007 *Polym. Rev.* **47** 197
[12] Sarkar B and Alexandridis P 2015 *Prog. Polym. Sci.* **40** 33
[13] Yan Y, Zhang J, Ren L and Tang C 2016 *Chem. Soc. Rev.* **45** 5232
[14] Tokareva I, Minko S, Fendler J H and Hutter E 2004 *J. Am. Chem. Soc.* **126** 15950
[15] Balazs A C, Emrick T and Russell T P 2006 *Science* **314** 1107
[16] Merlitz H, He G L, Wu C X and Sommer J U 2009 *Phys. Rev. Lett.* **102** 115702
[17] Mahboobeh Y, Alireza S and Mohammad K 2022 *J. Mol. Liq.* **362** 119732
[18] Knetsch M L W and Koole L H 2011 *Polymers* **3** 340
[19] Kim J U, O'Shaughnessy B 2006 *Macromolecules* **39** 413
[20] Halperin A, Fragneto G, Schollier A and Sferrazza M 2007 *Langmuir* **23** 10603
[21] Kim J U and Matsen M W 2008 *Macromolecules* **41** 246
[22] Hore M J A and Composto R J 2012 *Macromolecules* **45** 6078
[23] Ginzburg V V 2017 *Macromolecules* **50** 9445
[24] Sgouros A P, Revelas C J, Lakkas A T and Theodorou D N 2022 *J. Phys. Chem. B* **126** 7454
[25] Cao D and Wu J 2007 *J. Chem. Phys.* **126** 144912
[26] Striolo A and Egorov S A 2007 *J. Chem. Phys.* **126** 014902
[27] Verso F L, Yelash L, Egorov S A and Binder K 2011 *J. Chem. Phys.* **135** 214902
[28] Bakhshandeh A, Segala M and Escobar Colla T 2021 *Macromolecules* **55** 35
[29] Tai C H, Pan G T and Yu H Y 2019 *Langmuir* **35** 16835
[30] Mei X, Xie F, Song B, Guo Q and Jiao X 2025 *Chin. Phys. B* **34** 058902
[31] Merlitz H, Wu C X and Sommer J U 2012 *Macromolecules* **45** 8494
[32] Li Y, Kröger M and Liu W K 2014 *Biomaterials* **35** 8467
[33] Cheng J, Vishnyakov A and Neimark A V 2015 *J. Chem. Phys.* **142** 034705
[34] Gu C, Coalson R D, Jasnow D and Zilman A 2017 *J. Phys. Chem. B* **121** 6425
[35] Modica K J, Martin T B and Jayaraman A 2017 *Macromolecules* **50** 4854
[36] Cheng S, Stevens M J and Grest G S 2017 *J. Chem. Phys.* **147** 224901
[37] Santo K P, Vishnyakov A, Brun Y and Neimark A 2018 *Langmuir* **34** 1481
[38] Zhang L, Becton M D, Liu N, Averett R D, Pidaparti R M and Wang X 2019 *J. Chem. Theory Comput.* **15** 6382
[39] Gao H M, Li B, Zhang R, Sun Z Y and Lu Z Y 2020 *J. Chem. Phys.* **152** 094905
[40] Kim J U and O'Shaughnessy B 2002 *Phys. Rev. Lett.* **89** 238301
[41] Yaneva J, Dimitrov D I, Milchev A and Binder K 2009 *J. Colloid Interface Sci.* **336** 51
[42] Guskova O A, Pal S and Seidel C 2009 *Europhys. Lett.* **88** 38006
[43] Milchev A, Dimitrov D I and Binder K 2010 *Biomicrofluidics* **4** 032202
[44] Eisenriegler E, Hanke A and Dietrich S 1996 *Phys. Rev. E* **54** 1134
[45] Milchev A, Dimitrov D I and Binder K 2008 *Polymer* **49** 3611
[46] Sarkar B and Alexandridis P 2015 *Prog. Polym. Sci.* **40** 33
[47] Dai X, Hou C, Xu Z, Yang Y, Zhu G, Chen P and Yan L T 2019 *Entropy* **21** 186
[48] Muthukumar M 2012 *Adv. Chem. Phys.* **149** 129
[49] Dutta S and Benetatos P 2020 *Soft Matter* **16** 2114
[50] Hendricks J, Kawakatsu T, Kawasaki K and Zimmermann W 1995 *Phys. Rev. E* **51** 2658
[51] Gholami A, Wilhelm J and Frey E 2006 *Phys. Rev. E* **74** 041803
[52] Dutta S and Benetatos P 2018 *Soft Matter* **14** 6857
[53] Bayati P, Ghassab L and Najafi A 2014 *Eur. Phys. J. E* **37** 91
[54] Kratky O and Porod G 1949 *Recl. Trav. Chim. Pays-Bas* **68** 1106
[55] Jie Z and Laurence B 2025 *Phys. Rev. Lett.* **134** 218101
[56] DeTeresa S J , Porter R S and Farris R J 1985 *J. Mater. Sci.* **20** 1645
[57] Israels R, Leermakers F A M, Fleer G J and Zhulina E B 1994 *Macromolecules* **27** 3249
[58] Naji A, Seidel C and Netz R R 2005 *Theoretical approaches to neutral and charged polymer brushes December* **20** 2005
[59] Wijmans C M, Leermakers F A M and Fleer G J 1994 *J. Chem. Phys.* **101** 8214
[60] Egorov S A, Hsu H P, Milchev A and Binder K 2015 *Soft Matter* **11** 2604